Exchange-Induced Anisotropies at Ferromagnetic-Antiferromagnetic Interfaces above and below the Néel Temperature

M. Grimsditch and A. Hoffmann
Materials Science Division, Argonne National Laboratory, Argonne, Illinois 60439, USA

P. Vavassori
INFM UdR of Ferrara-Dipartimento di Fisica, Universita di Ferrara, Ferrara, Italy, and INFM-National Research Center on nanoStructures and Biosystems at Surfaces (S^3), Ferrara, Italy

Hongtao Shi and D. Lederman
Department of Physics, West Virginia University, Morgantown, West Virginia 26506-6315, USA
(Received 23 January 2003; published 24 June 2003)

The exchange bias and magnetic anisotropies in a Co layer on a single-crystalline FeF_2 film have been determined between 30 and 300 K. By postulating that the coupling between the ferromagnet and the antiferromagnet persists above the Néel temperature (T_N) we develop a model that quantitatively describes the exchange bias and the anisotropies over the whole temperature range, both above and below T_N. Using only the measured low temperature exchange bias and a distribution of blocking temperatures we explain (i) the temperature dependence of the bias, (ii) the magnitude of the anisotropies, (iii) the opposite sign of the first and second order anisotropies, (iv) the observed $1/T$ and $1/T^3$ temperature dependencies of the first and second order uniaxial anisotropies above T_N, and (v) the decrease of the anisotropies below T_N.

DOI: 10.1103/PhysRevLett.90.257201 PACS numbers: 75.70.Cn, 75.60.Ej

The interaction at an interface between an antiferromagnet and a ferromagnet gives rise to exchange bias, which manifests itself as a shift of the ferromagnetic hysteresis loop. Even though this effect was discovered almost half a century ago [1], there are ongoing controversies about the underlying mechanism [2,3]. The continued interest in this phenomenon is also augmented by its widespread use in magnetic technology for establishing a reference magnetization direction [4].

Besides the shift of the hysteresis loop, the coupling at the ferromagnet/antiferromagnet interface generally also gives rise to an enhancement of the coercivity [2]. This suggests that the interface interaction introduces anisotropies above and beyond the unidirectional anisotropy responsible for the exchange bias. The coercivity enhancement has recently attracted increased attention since, ultimately, both the coercivity and the exchange bias contain information about the fundamental coupling mechanism between the ferromagnet and the antiferromagnet. Most well-controlled experiments have been performed in layered exchange bias systems and it has been observed that the ferromagnetic and the antiferromagnetic layer thicknesses determine the magnitude of the coercivity enhancement [5,6] as well as its temperature dependence [7].

Several theoretical models have been proposed to explain the observed coercive behavior. These models include spin-flop coupling where the magnetization direction of the ferromagnet aligns preferentially perpendicular to the antiferromagnetic anisotropy axis [8], random field interactions [9], or magnetic frustration [7], which lead to domain wall pinning, or reversible and irreversible changes in the antiferromagnetic domain structure [10]. In particular, in the latter framework, temperature-dependent effects in the coercivity have been explained by thermal instabilities of the antiferromagnetic state similar to superparamagnetism [11]. It should be pointed out that all the proposed models so far deal only with the properties of exchange bias systems below the Néel temperature of the antiferromagnet. It has been observed previously, however, that exchange bias systems with single-crystalline FeF_2 as the antiferromagnet show a coercivity enhancement with a peak at the blocking temperature (coinciding in this case with the Néel temperature $T_N = 78$ K), which extends well above the bulk ordering temperature of FeF_2 [12–15].

Here we present measurements of a Co film grown on a single-crystalline FeF_2 film. Easy-axis magnetization loops reproduce the previously observed exchange bias below T_N and the peak of the coercivity enhancement at the Néel temperature [12–15]. Because coercivity is a complex phenomenon that can depend on the functional form of the energy (i.e., shape and intrinsic anisotropies), temperature, defects, etc., we focus here on anisotropies extracted from the hard-axis hysteresis loops and verified with Brillouin light scattering. We then show that the observed temperature dependence of the first and second order uniaxial anisotropies above T_N can be explained with a simple model based on interactions of the ferromagnet with locally ordered regions within the antiferromagnet. A slight generalization of the model to include a range of blocking temperatures describes quantitatively

the unidirectional anisotropy and the uniaxial anisotropies over the whole temperature range.

The FeF_2/Co bilayer sample was grown on a single crystal MgF_2 (110) substrate via molecular beam epitaxy [15,16]. A 68-nm thick FeF_2 layer was first deposited on the substrate at 297 °C, followed by an 18 nm Co layer grown at 125 °C, which was capped by a 5 nm MgF_2 layer, grown at room temperature, to prevent oxidation of the Co film. A structural characterization of the Co film showed it to be polycrystalline with little or no texturing. The Curie temperature for an 18 nm Co film is expected to be close to that of bulk Co [17].

The hysteresis loops were measured in the transverse magneto-optic Kerr effect (MOKE) configuration [18] with the sample mounted on the cold finger of a cryostat placed between the poles of an electromagnet. This arrangement enabled Brillouin spectra and MOKE measurements to be recorded under identical conditions.

In Fig. 1 we show easy- and hard-axis loops at four representative temperatures T (300, 95, 69, and 29 K), after cooling the sample with a 2 kOe field applied along the c axis of the single-crystalline FeF_2 antiferromagnetic layer. This cooling field direction corresponds to the easy axis of the Co layer. The easy-axis loops (right column) reproduce the results in earlier reports showing a maximum in the coercivity at T_N and the gradual appearance of the exchange bias below T_N [12–15]. The hard-axis loops (left column), which were measured with the field applied in plane but perpendicular to the cooling field, also show significant changes down to T_N but change little below this temperature. We show below that although the hard-axis loops do not change shape below T_N the interplay between exchange bias and anisotropy leads to a decrease in the magnitude of the anisotropies as T is lowered below T_N.

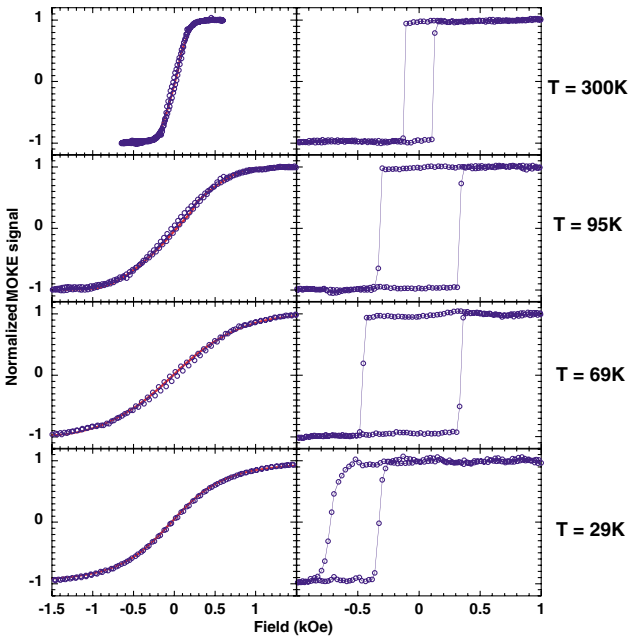

FIG. 1 (color online). Hysteresis loops with the field applied perpendicular (hard axis) and parallel (easy axis) to the FeF_2 c axis at various temperatures. The lines for the hard-axis data are fits using a coherent rotation model and the energy expression from Eq. (1), while the lines for the easy axis data are just guides to the eye.

The hard-axis hysteresis loops were fit with a coherent rotation model to the energy density (divided by the saturation magnetization M_F)

$$E/M_F = -H\cos(\theta - \theta_H) + H_E\cos(\theta) + (K_1/M_F)\cos^2(\theta) + (K_2/M_F)\cos^4(\theta), \quad (1)$$

where H is the applied field, θ and θ_H are the (in-plane) angles the magnetization of the Co layer and the applied field subtend with the FeF_2 c axis, respectively, H_E is the exchange bias, and K_1 and K_2 are, respectively, first and second order uniaxial anisotropies of the ferromagnet. The hard-axis loops were fitted with the uniaxial anisotropies as free parameters and H_E determined from the easy-axis loops. As can be seen from the excellent fits to the data in Fig. 1, the energy given by Eq. (1) provides a very good description of the hysteresis loops. It should be noted that the anisotropy values extracted from the hard axis qualitatively reproduce the coercivity trends of the easy-axis loops. However, the coercivities extracted from the coherent rotation model for the easy-axis loops are a factor of 2 larger, probably an indication that the easy-axis magnetization reversal mechanism is not a simple coherent rotation.

In Fig. 2 we have plotted (symbols) the parameters extracted from the fits to the hysteresis loops. Worthy of note are (i) the strong temperature dependence of the anisotropies above T_N (much larger than for pure Co), (ii) the change in the evolution of the anisotropies near T_N (if the anisotropies were induced by a thermal

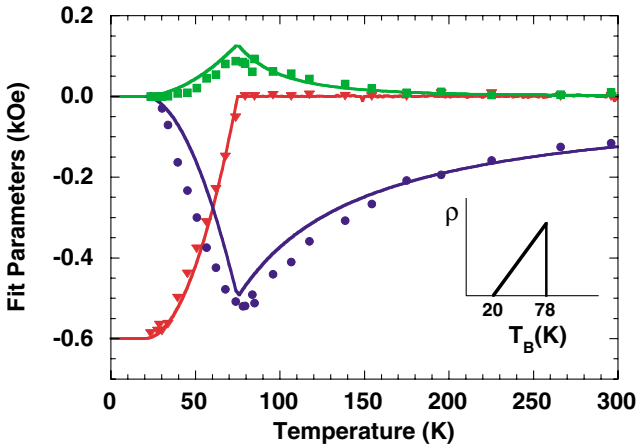

FIG. 2 (color online). Parameters extracted from fitting the hysteresis curves (symbols); H_E (▼), K_1/M_F (●), and K_2/M_F (■). The full lines are the model calculations using Eq. (8). The inset shows the distribution of blocking temperatures used for the calculations.

expansion mismatch, there appears to be little reason for the change in behavior at T_N), and (iii) the opposite sign of K_1 and K_2.

In order to ascertain that Eq. (1) is indeed the "correct" energy expression (and not just one of many expressions that might reproduce the data), we have performed Brillouin scattering experiments. Our experimental Brillouin data are in good agreement with the frequencies calculated based on Eq. (1) and the parameters in Fig. 2. This confirms that our chosen energy expression provides a self-consistent description of both the static and dynamic properties of our exchange coupled system both above and below T_N.

The temperature dependence of the anisotropies of the Co film can be understood, by assuming that the ferromagnet is still coupled to the antiferromagnet above its bulk Néel temperature. This is a reasonable assumption given that the net exchange interaction at the antiferromagnetic/ferromagnetic interface could cause local ordering at the surface of the antiferromagnet, in the same way that an external field causes a ferromagnet to order at a temperature greater than its Curie temperature. It has been recently shown theoretically that such a coupling would lead to a significant coercivity enhancement well above T_N [19]. Furthermore, there is also experimental evidence for ordering of the antiferromagnet above its bulk Néel temperature when it is exchange coupled to another magnetically ordered system [20].

The interface coupling energy per unit area in an exchange bias system between a ferromagnet (F) and an antiferromagnet (AF) can be written as

$$E_{\mathrm{ex}} = -\langle J M_{\mathrm{F}} M_{\mathrm{AF}} \cos(\theta')\rangle_{\mathrm{int}}, \tag{2}$$

where J is the strength of the coupling, θ' is the angle between the ferromagnetic magnetization and the antiferromagnetic sublattice orientation, and the brackets denote an average over the interface (i.e., over both sublattices). As a result of the large single-ion magnetic anisotropy in FeF_2, we assume that the sublattice magnetization in the AF has only two possible orientations, viz., along the FeF_2 c axis. Consequently θ' in Eq. (2) becomes equivalent to θ in Eq. (1). If we assume a homogeneous magnetization in the ferromagnet, implicit in the coherent rotation model, then Eq. (2), can be simplified to

$$E_{\mathrm{ex}} = -J_{\mathrm{int}} \cos(\theta), \tag{3}$$

with $J_{\mathrm{int}} = M_{\mathrm{F}}\langle J M_{\mathrm{AF}}\rangle_{\mathrm{int}}$. J_{int} can be nonzero even for a nominally compensated antiferromagnet interface, either because the ferromagnet couples preferentially to one of the AF sublattices via uncompensated spins (so that $\langle M_{\mathrm{AF}}\rangle_{\mathrm{int}} \neq 0$) or if the coupling constant is different for each sublattice site. This latter case may be particularly significant for FeF_2 [110] surfaces where the two Fe sublattices are inequivalent: one sublattice has its F ions in the plane, the other perpendicular to the plane [21]. We postulate that, even above T_N, the same functional form for the coupling between the ferromagnet and the ordered interfacial antiferromagnetic spins is maintained.

Following the approach of Ref. [19], the free energy, based on the interfacial energy in Eq. (3), can be evaluated. If we assume that at high temperatures the two possible orientations are in thermal equilibrium, their population levels are given by

$$f^{\pm} = \frac{e^{\pm (T_0/T)\cos(\theta)}}{e^{(T_0/T)\cos(\theta)} + e^{-(T_0/T)\cos(\theta)}}, \tag{4}$$

where $T_0 = J_{\mathrm{int}} A/k_B$ and A is the interface area of the AF domain. The interface free energy thus becomes

$$\begin{aligned} F_{\mathrm{int}} &= -J_{\mathrm{int}} \cos(\theta)(f^+ - f^-) \\ &= -J_{\mathrm{int}} \cos(\theta) \tanh\left[\frac{T_0}{T}\cos(\theta)\right]. \end{aligned} \tag{5}$$

Well below T_N, where, for a field cooled sample $f^+ = 1$ and $f^- = 0$, we recover the usual expression for the unidirectional exchange bias at $T = 0$ with $H_E(0) = -J_{\mathrm{int}}/dM_{\mathrm{F}}$, where d is the thickness of the ferromagnetic film. Above T_N, where the AF domains are thermally activated, a high temperature expansion of Eq. (5) leads to the free energy

$$F_{\mathrm{int}} = -\frac{T_0}{T} J_{\mathrm{int}} \cos^2(\theta) + \frac{1}{3}\left(\frac{T_0}{T}\right)^3 J_{\mathrm{int}} \cos^4(\theta). \tag{6}$$

We note that the accuracy of the expansion, keeping only up to T^{-3} terms, is 10% at T_0 and improves at higher T. A comparison of Eqs. (1) and (6) allows us to identify

$$K_1/M_F = +H_E(0)\frac{T_0}{T} \quad \text{and} \tag{7a}$$

$$K_2/M_F = -\frac{H_E(0)}{3}\left(\frac{T_0}{T}\right)^3. \tag{7b}$$

The model thus correctly predicts both sign and magnitude of K_1 and K_2 shown in Fig. 2. Furthermore, K_1 and K_2 should exhibit a $1/T$ and $1/T^3$ dependence, respectively. Taking $H_E = 0.6$ kOe, as determined from the lowest temperature easy-axis loops, and choosing $T_0 = 68$ K indeed provides a good description of the anisotropies and their T dependence above T_N.

The high temperature dependence described above is valid if all the AF domains are free to reorient and reach their thermal equilibrium distribution during the measurement time. The temperature at which they no longer reach their equilibrium is known as the blocking temperature T_B. At this temperature exchange bias sets in and it has been shown by Fulcomer and Charap that a distribution of T_B's can provide the correct temperature dependence of H_E [11]. T_B depends on the anisotropy energy of each antiferromagnetic domain and hence, similar to T_0, is proportional to the interface area of each domain. Using reasonable values of the material parameters of our film it can be estimated that $1/3 < T_0/T_B < 3$.

Thus, at a given temperature T, AF domains with $T_B < T$ contribute only to the anisotropies while domains

with $T_B > T$ contribute only to the bias. For a distribution $\rho(T_B)$ of blocking temperatures we expect the exchange bias and the anisotropies to be given by

$$H_E(T) = H_E(0)\left[1 - \int_0^T \rho(T_B)dT_B\right], \quad (8a)$$

$$K_1(T)/M_F = \frac{H_E(0)}{T}\int_0^T T_0\rho(T_B)dT_B, \quad \text{and} \quad (8b)$$

$$K_2(T)/M_F = -\frac{H_E(0)}{3T^3}\int_0^T T_0^3\rho(T_B)dT_B. \quad (8c)$$

To carry out the last two integrals we have chosen $T_0/T_B = 1.1$; larger values improve the agreement for K_1 but make the agreement for K_2 worse.

It turns out that the distribution of blocking temperatures (ρ) is not critical. We have tested numerous distributions:, e.g., $\rho =$ const in the range $35 < T_0 < 78$ K and zero outside this range, a quadratically increasing density with its cut off at 78 K and two linearly increasing distributions both with a maximum at 78 K but starting at 0 and 20 K, respectively. The latter choice, shown in the inset to Fig. 2, produces marginally better agreement and results in the full lines in Fig. 2.

We emphasize the assumptions entering the model that lead to the full lines in Fig. 2: (i) an interface interaction independent of temperature, (ii) all values are scaled to the measured low temperature exchange bias, (iii) a distribution of ''blocking'' temperatures, and (iv) a fit parameter relating the blocking temperature to T_0. Given these very simple premises, the agreement between the experimental results and the model predictions are remarkable.

Although it is difficult to assess the applicability of the present model to all previously studied F/AF systems, there are some discernible consequences in the case of previously studied twinned (110) FeF_2 samples. The first order anisotropies from the two twins should lead to an average, isotropic term (which can be ignored), while the second order anisotropies should have the functional form $K_2 \propto [\sin^4(\theta) + \cos^4(\theta)]$ and, because the sign of K_2 is opposite to that of K_1, the easy axis should be 45° to the c axes. The latter assertion is known to be correct in the case of Fe on FeF_2 [14] and Co on FeF_2 and $Fe_xZn_{1-x}F_2$ [15]. Furthermore, since $K_2 < K_1$, the coercivity enhancement at T_N should be smaller for twinned or polycrystalline samples, which is again in agreement with earlier measurements [14,15]. Similarly we would expect the induced anisotropies to be smaller and, conversely, the coercivity enhancement to be reduced for nonuniaxial antiferromagnets, such as CoO or FeMn.

In summary, we have shown that large magnetic anisotropies are induced in a ferromagnetic film deposited on an antiferromagnetic substrate even well above the Néel temperature of the antiferromagnet. We interpret our results as due to the short-range order induced in the antiferromagnet by the ferromagnet. Above T_N our model explains the magnitude, sign, and temperature dependence of the first and second order anisotropies using only the measured maximum exchange bias and a single blocking temperature. Below T_N a distribution of blocking temperatures is needed to explain both the anisotropies and the exchange bias. The good agreement between the model predictions and the experimental results provides strong evidence that the underlying assumptions of the model are indeed correct.

We acknowledge many insightful discussions with Chris Leighton and Thomas Schulthess. Work at ANL supported by the U.S. DOE-BES under Contract No. W-31-109-ENG-38. Work at WVU supported by the U.S. DOE-BES under Grant No. DE-FG45862 and the U.S. NSF under Grant No. EPS-0083046.

[1] W. H. Meiklejohn and C. P. Bean, Phys. Rev. **102**, 1413 (1957).
[2] J. Nogués and I. K. Schuller, J. Magn. Magn. Mater. **192**, 203 (1999).
[3] A. E. Berkowitz and K. Takano, J. Magn. Magn. Mater. **200**, 552 (1999).
[4] J. C. S. Kools, IEEE Trans. Magn. **32**, 3165 (1996).
[5] R. Jungblut, R. Coehoorn, M. T. Johnson, J. aan de Steege, and A. Reinders, J. Appl. Phys. **75**, 6659 (1994).
[6] C. Leighton, M. R. Fitzsimmons, A. Hoffmann, J. Dura, C. F. Majkrzak, M. S. Lund, and I. K. Schuller, Phys. Rev. B **65**, 064403 (2002).
[7] C. Leighton, J. Nogués, B. J. Jönsson-Åkerman, and I. K. Schuller, Phys. Rev. Lett. **84**, 3466 (2000).
[8] T. C. Schulthess and W. H. Butler, Phys. Rev. Lett. **81**, 4516 (1998).
[9] Z. Li and S. Zhang, Phys. Rev. B **61**, R14 897 (2000).
[10] M. D. Stiles and R. D. McMichael, Phys. Rev. B **63**, 064405 (2001).
[11] E. Fulcomer and S. H. Charap, J. Appl. Phys. **43**, 4190 (1972).
[12] T. J. Moran, J. Nogués, D. Lederman, and I. K. Schuller, Appl. Phys. Lett. **72**, 617 (1998).
[13] J. Nogués, T. J. Moran, D. Lederman, I. K. Schuller, and K. V. Rao, Phys. Rev. B **59**, 6984 (1999).
[14] M. R. Fitzsimmons *et al.*, Phys. Rev. B **65**, 134436 (2002).
[15] H. Shi and D. Lederman, Phys. Rev. B **66**, 094426 (2002).
[16] H. Shi, D. Lederman, and E. E. Fullerton, J. Appl. Phys. **91**, 7763 (2002).
[17] F. Huang, M. T. Kief, G. J. Mankey, and R. F. Willis, Phys. Rev. B **49**, 3962 (1994).
[18] O. Cugat, D. Givord, J. P. Rebouillat, and Y. Souche, J. Magn. Magn. Mater. **104**, 397 (1992).
[19] C. Leighton, H. Suhl, M. J. Pechan, R. Compton, J. Nogués, and I. K. Schuller, J. Appl. Phys.. **92**, 1483 (2002).
[20] P. J. van der Zaag, Y. Ijiri, J. A. Borchers, L. F. Feiner, R. M. Wolf, J. M. Gaines, R. W. Erwin, and M. A. Verheijen, Phys. Rev. Lett. **84**, 6102 (2000).
[21] M. Weissmann, A. M. Llois, and M. Kiwi, J. Magn. Magn. Mater. **234**, 19 (2001).